Fast Selection of Bidirectional Turbines for Oscillating Water Column Systems from a Catalogue of Turbine Types

T.H. Carolus[1], C. Moisel[1], R. Starzmann[2]

[1]*Institute for Fluid- and Thermodynamics, University of Siegen. 57068 Siegen, Germany*

[2]now with *SCHOTTEL HYDRO GmbH, Mainzer Straße 99, 56322 Spay, Germany*

Corresponding author: thomas.carolus@uni-siegen.de

***Abstract*— A collector of an oscillating water column system (OWC) for wave energy utilization requires a bidirectional turbine that copes with a nominal pneumatic power while providing a specified impedance or, in terms of an OWC designer, "damping". The damping is realized by the slope of the flow rate vs. pressure head performance curve of the turbine chosen. Often it is common practice to take a standard turbine type - for instance a particular design of the well-known Wells turbine. With the number of bidirectional turbine designs increasing designers of OWC systems are facing more options to select and dimension a turbine. Energy yield, size and hence cost of the turbine and electric generator, operational behaviour, envisaged control strategy and noise emitted by the turbine may be criteria for selection.**

Objective of this paper is to describe a simple strategy how to make a first choice of a turbine from a catalogue of different turbine types for a particular application. Starting point is the set of non-dimensionalized steady-state characteristics of each turbine in the catalogue. Utilizing standard scaling laws and a simplistic time domain model for the cyclic turbine operation, turbine size and rotor speed, number for stages or flows, and performance curves can be determined. Examples illustrate the application of the method.

***Keywords*— Bidirectional Air Turbine, Oscillating Water Column, Wave Energy**

I. INTRODUCTION

The principle of an oscillating water column (OWC) is used in power plants which extract the energy of ocean waves and convert it into shaft power of a bidirectional air turbine, Fig. 1. p is the static gauge pressure inside of the collector (with reference to the constant barometric pressure p_b outside in the free atmosphere). It is oscillating with time according to the water surface wave motion and the dynamic properties of the complete OWC-system and causes a volume flow rate $\dot{V}$ through an upper opening. Typically the designer of an OWC specifies an impedance of the upper opening (often called the 'damping')

$$D_{ts} = \frac{p}{\dot{V}} \qquad (1)$$

that ensures maximum available pneumatic power

$$P_{p,avail}(t) = \dot{V}(t) \cdot p(t) \qquad (2)$$

at a specified sea state (i.e. amplitude of wave height and mean wave period). If the collector is large as compared to the size of the turbine, for the most part of the collector the velocity of air is negligibly small. Hence, p is equivalent to the total-to-static pressure head Δp_{ts} which is seen by a turbine placed at the upper opening.

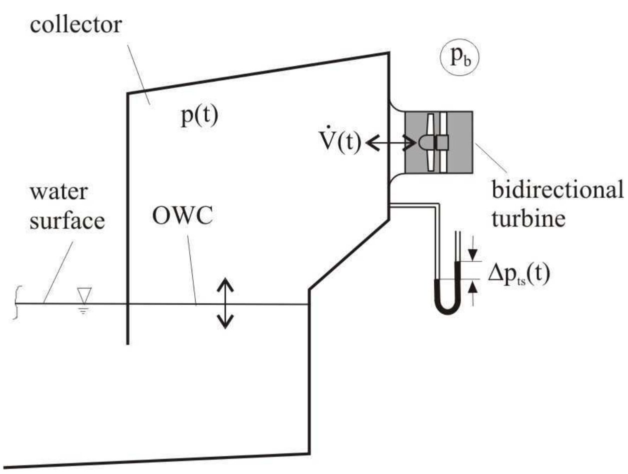

Fig. 1. Oscillating water column system (schematically).

Designers of early OWC power plants were unable to choose among a large variety of types of bidirectional turbines. In some cases this led to mistuned OWC-systems, because the turbine was 'over-damping' or vice versa. This has changed over the past years. The classical axial Wells turbine [1], i.e. a reaction turbine requiring airfoil-type blades with their lift being a key parameter, or in other words a 'lift-based' turbine, experienced the most research and development efforts during the past 40 years, see e.g. Raghunathan [2] and a couple of more recent contributions by the authors of this present paper ([3] - [8]). The reaction working principle has even been applied to radial and mixed-flow (i.e. diagonal) turbine rotors [9], [10]. As an alternative a zero-reaction, so-called 'impulse type' turbine for bidirectional flow, originally invented by Babinstev [11], is under investigation. Recent overviews on bidirectional air turbines for use in OWCs have been published by Setoguchi and Takao [12], Falcão and Gato [13] and Curran and Folley [14].

In summary it may be concluded that designers of modern OWC systems are facing many more options to select a turbine type than in the past. Inherently this leads to the question how to dimension and operate a specific type of turbine to achieve best overall performance in an application. This paper is mainly addressed to system designer. We will show a simple

ISSN 2309-1983

method for making a first choice of turbine type, size and rotor speed and the number of turbines in series or parallel required. Starting point are sets of non-dimensional steady-state characteristics of various turbine types. Typically, those data come from model scale laboratory tests but full scale data can be used, too. Possible criteria for selection are maximum energy yield, turbine size, limits of noise emission and the envisaged control strategy.

For simplicity, in this paper we aim at turbines for maximum energy yield for one specified sea state. The turbine operation is assumed to be fixed rotational speed. The acoustic performance is not included in this paper, for that we refer e.g. to [5].

II. Turbine Selection Scheme

A. Non-dimensional characteristics

Starting point is a set of accurately measured characteristics of a type of turbine in terms of non-dimensional performance coefficients. We prefer the widely used flow rate, pressure head and shaft power coefficient

$$\phi \equiv \frac{\dot{V}}{\frac{\pi^2}{4} d^3 n}, \tag{3}$$

$$\psi_{ts} \equiv \frac{\Delta p_{ts}}{\frac{\pi^2}{2} d^2 n^2 \rho}, \tag{4}$$

$$\lambda \equiv \frac{P_{shaft}}{\frac{\pi^4}{8} d^5 n^3 \rho}. \tag{5}$$

d is the characteristic rotor diameter (usually the outer diameter), n its rotational speed, ρ the mean density of the air through the turbine.

Fig. 2 shows schematically a set of non-dimensional characteristics. Coming from zero pressure head the onset of the desired shaft power is at $\psi_{ts,0}$ - not at $\psi_{ts} = 0$ because of internal losses. The shaft power increases with pressure head up to the stall point. There the shaft power is maximal. Beyond stall (i.e. $\psi_{ts,mp}$) the flow rate abruptly increases substantially while the shaft power drops towards 0. Details of the stalled operational regime are not shown in Fig. 2. At least for most of the lift-based type of turbines the volume flow rate through the turbine increases in very good approximation linearly with pressure head up to the stall point.

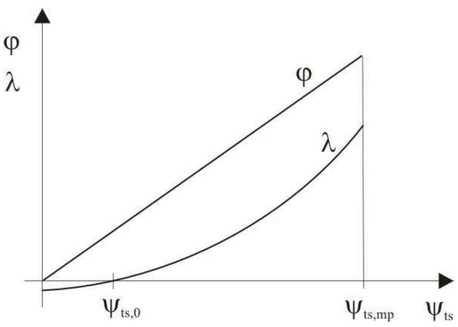

Fig. 2. Aerodynamic non-dimensional steady-state characteristics of a bidirectional turbine (schematically).

B. Simplistic time domain model

In the collector the static pressure varies cyclically with time as

$$p(t) = \hat{p}\, sin\, \omega t = \hat{p}\, sin \frac{2\pi}{T_m} t\,. \tag{6}$$

$\hat{p}$ is the amplitude, T_m the period of the oscillation. Since the collector requires a specified value of the damping D_{ts}, the volume flow rate through the upper opening in Fig. 1 must be adjusted to

$$\dot{V}(t) = \hat{\dot{V}}\, sin\, \omega t = \hat{p}\, sin \frac{2\pi}{T_m} t \quad \text{with} \quad \hat{\dot{V}} = \frac{\hat{p}}{D_{ts}}\,. \tag{7}$$

Placing a turbine in the upper opening the pressure head $\Delta p_{ts}(t)$, as seen by the turbine, equals $p(t)$, whereas $\dot{V}(t)$ is the volume flow rate the turbine must take, i.e. its 'swallowing capacity'. Fig. 3 shows schematically the cyclically varying pressure in the collector $p(t)$ which equals the argument Δp_{ts} in the turbine performance curves $\dot{V} = f(\Delta p_{ts})$ and $P_{shaft} = f(\Delta p_{ts})$.

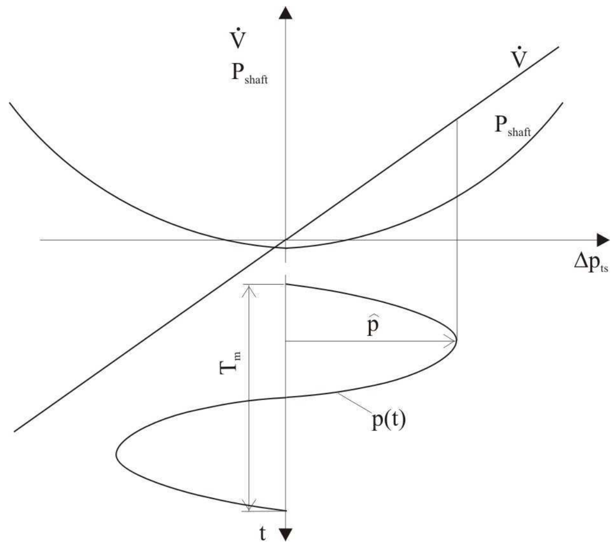

Fig. 3. Steady-state performance curves of a turbine with D and n = const. and sinusoidally varying pressure head (schematically).

For any pair of values d and n the turbine performance curves can be computed by inverting eqs. (3) and (4). d and n, however, are unknowns so far. Hence, we propose a strategy as follows:

- Select a test design point ($\psi_{ts,DP}$, φ_{DP}) on the non-dimensional characteristics.
- As a key assumption in this scheme set the turbine design power $\Delta p_{ts,DP} \dot{V}_{DP}$ as the peak power $\hat{p}\hat{\dot{V}}$ available from the collector. By doing so, $\Delta p_{ts,DP}$ and $\dot{V}_{DP}$ are known.
- Calculate d and n from eqs. (3) and (4):

$$d = \sqrt[4]{\frac{8\rho}{\pi^2} \frac{\psi_{ts,DP}}{\varphi_{DP}^2} \frac{\dot{V}_{DP}^2}{\Delta p_{ts,DP}}} \tag{8}$$

$$n = \frac{4}{\pi^2} \frac{\dot{V}_{DP}}{\varphi_{DP} d^3} \tag{9}$$

- With d and n known calculate the performance curve $\dot{V} = f(\Delta p_{ts})$ which now runs exactly through $(\hat{p}, \hat{\dot{V}})$, and $P_{shaft} = f(\Delta p_{ts})$.

- Compute the instantaneous shaft power $P_{shaft}(t)$ and determine the energy yield for a half wave

$$W_{shaft} = \int_0^{T_m/2} P_{shaft}(t)\,dt \,. \tag{10}$$

- An average efficiency of the energy transformation from the collector to the turbine shaft is defined as

$$\eta_{av} \equiv \frac{W_{shaft}}{W_p} = \frac{\int_0^{T_m/2} P_{shaft}(t)\,dt}{\int_0^{T_m/2} P_{p,avail}(t)\,dt} \,. \tag{11}$$

- Repeat all steps for a number of other test design points in the range $\psi_{ts} \le \psi_{ts,DP} \le \psi_{ts,mp}$ and search for the one with maximum energy yield or, equivalently, maximum average efficiency η_{av}. d_{opt} and n_{opt} for this optimum design point are the preferred turbine parameters.

- Calculate the circumferential Mach number

$$Ma = \frac{\pi d n}{c_0} \tag{12}$$

(with e.g. a typical value of the speed of sound c_0 = 346 m/s). Since operation of a turbine at a too large Mach number degrades its performance substantially, reject results in case the Mach number exceeds a set critical value (e.g. 0.5).

III. Examples

A. Selection of turbines from a catalogue of turbine types

With this example we demonstrate the procedure of turbine selection from an existing catalogue of various turbine designs. We consider two different OWC-collector scenarios: The 'design' pneumatic power, available from both collectors, shall be equal and is quantified in terms of the peak power

$$\hat{P}_{p,avail} = \hat{\dot{V}} \cdot \hat{p} = 100 \text{ kW}.$$

Each collector, however, requires a different damping by the turbine and provides an oscillating pressure with the pressure amplitude accordingly, Tab. 1. The mean air density be ρ = 1.2 kg/m^3 in both scenarios.

Tab. 2 shows candidates of turbines, arbitrarily chosen from a huge data base of turbines developed and model-tested at the University of Siegen [15]. All are single-stage, single-flow turbines. Their non-dimensional characteristics are depicted, cp. Fig. 8 or 9.

Tab. 1. Given collector scenarios for the examples.

Collector scenario	D_{ts} [Pa/(m^3/s)]	$\hat{p}$ [Pa]
(a)	250	5,000
(b)	1,000	10,000

Tab. 2. Candidates of single-stage and single-flow bidirectional turbines considered in the examples (developed and performance tested at the University of Siegen [15])

B	Axial with low solidity rotor 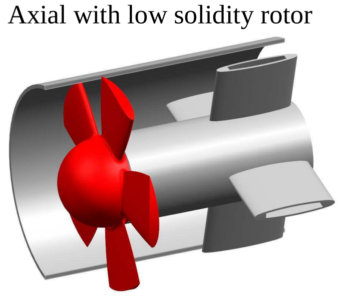	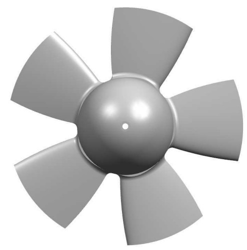
D	Axial with high solidity rotor 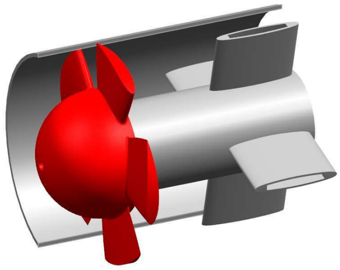	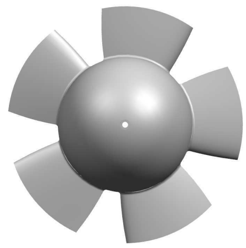
G	Axial with low solidity rotor and guide vanes 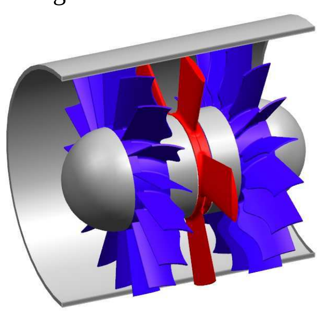	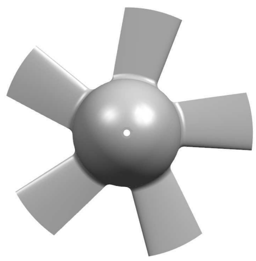
M	Mixed-flow 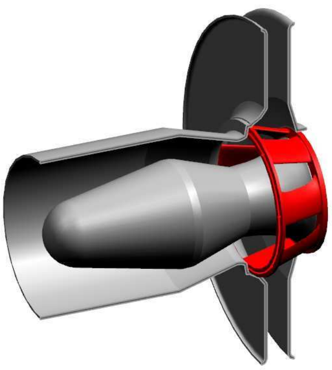	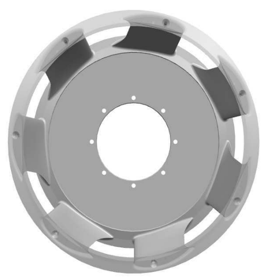

For illustration we consider turbine type D. We select five test design points as indicated in the upper graph of Fig. 4. For the collector scenario (a) each design point yields the necessary values of *D* and *n* and eventually the performance curves as in Fig. 5. As expected all performance curves $\dot{V} = f(\Delta p_{ts})$ meet Δp_{ts} = 5,000 Pa and $\dot{V}$ = 20 m^3/s, corresponding to the 'design' available pneumatic power of 100 kW. Fig. 6 shows a half cycle of pressure head input, the corresponding volume flow rate through the turbine, and the instantaneous shaft power. Of course the available instantaneous pneumatic power is independent of the design point tested, whereas the scatter of the shaft power indicates favourable or less favourable design points with respect to energy yield. As a summary, Fig. 7 depicts the results from all five test designs points. Clearly, a scale version of turbine D with *d* = 1.83 m, and operated at *n* = 1070 rpm will yield the maximum energy per half cycle. The maximum average efficiency is 55%. The circumferential Mach number is with 0.28 quite moderate.

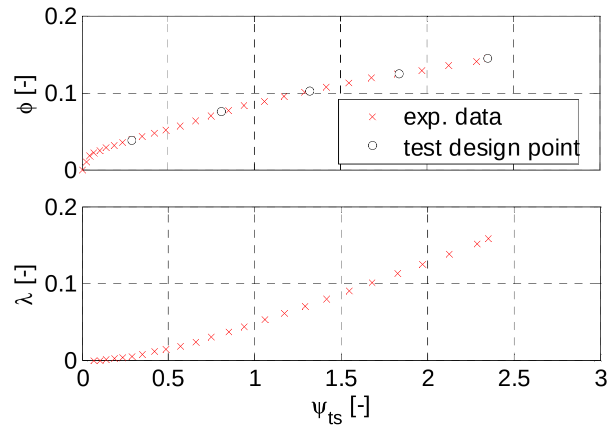

Fig. 4. Turbine D: Non-dimensional characteristics and five tested design points.

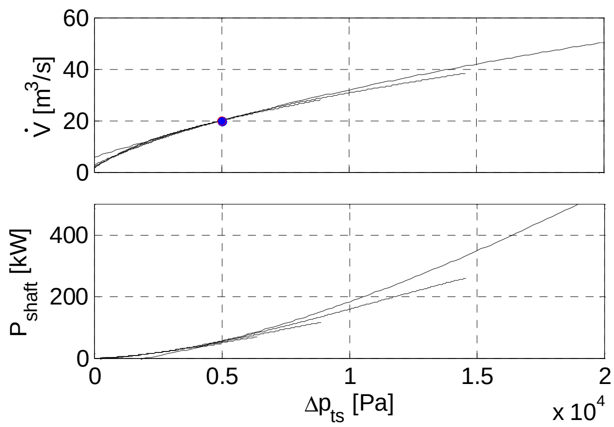

Fig. 5. Turbine D: Family of performance curves for the five design points tested; the marker corresponds to the available pneumatic power from the collector ('design' power).

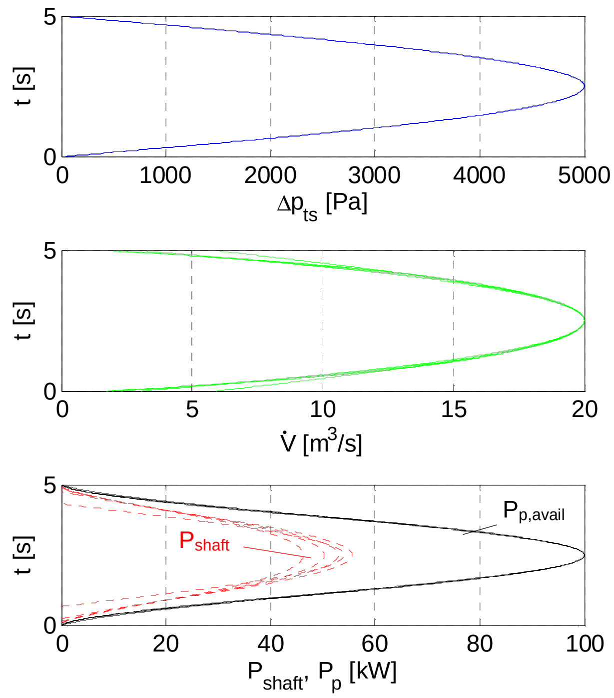

Fig. 6. Turbine D: Upper: Half cycle of pressure head input to the turbine; middle: volume flow rate through the turbine; lower: pneumatic power available from the collector and family of turbine shaft power according to the five design points tested.

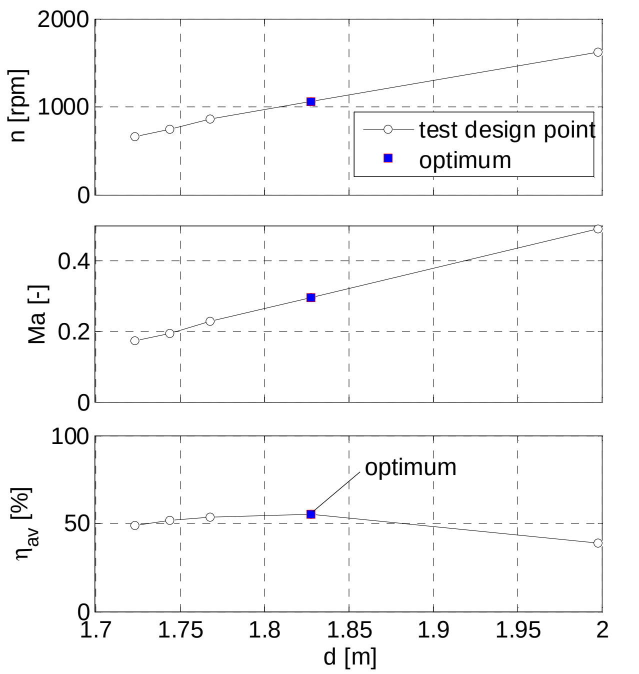

Fig. 7. Turbine D: Rotor diameter, rotational speed, circumferential Mach number and average efficiency for the five design points tested.

Eventually this process is repeated for all candidates of turbines from our sample catalogue. The optimal design points are identified (Figs. 8 and 9) and the optimal values of *d* and *n* are determined accordingly (Fig. 10). Comparing the optimal design points in Fig. 8 with 9, it becomes evident that the collector-scenario itself has an important impact on the design point which is identified as optimum.

Let us discuss two extreme choices: Turbine D and G. The values in Tab. 3 show that turbine G operates with the largest average efficiency for both collector scenarios. The size of G is nearly half of D. In turn, turbine G needs to run much faster than D, in collector (b) for instance at 5170 rpm, while D at moderate 2550 rpm. But another criterion for turbine selection is of importance: D operates far away from the maximum

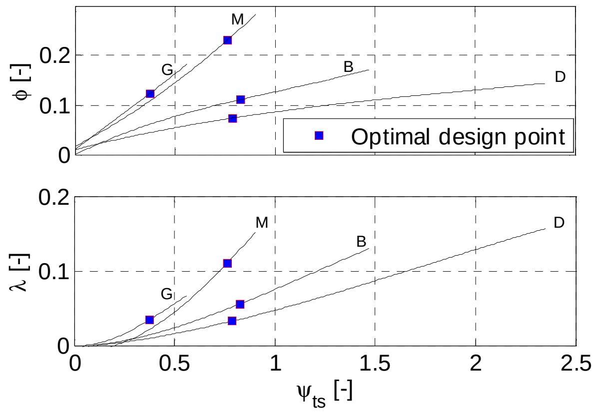

Fig. 8. Collector scenario (a) ('design' damping D_{ts} = 250 Pa/(m^3/s)): Optimal design points for all turbine types in the catalogue.

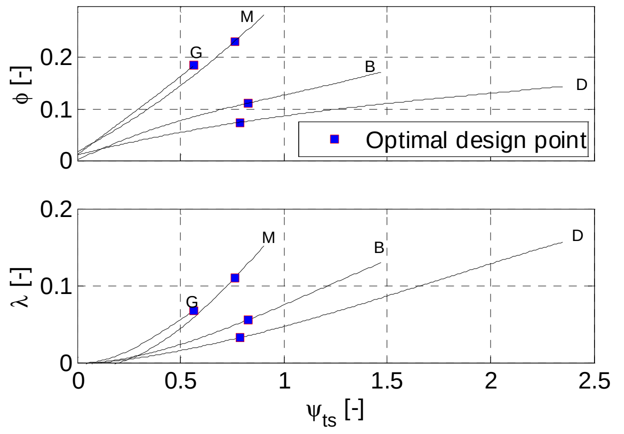

Fig. 9. Collector scenario (b) ('design' damping D_{ts} = 1,000 Pa/(m^3/s)): Optimal design points for all turbine types in the catalogue.

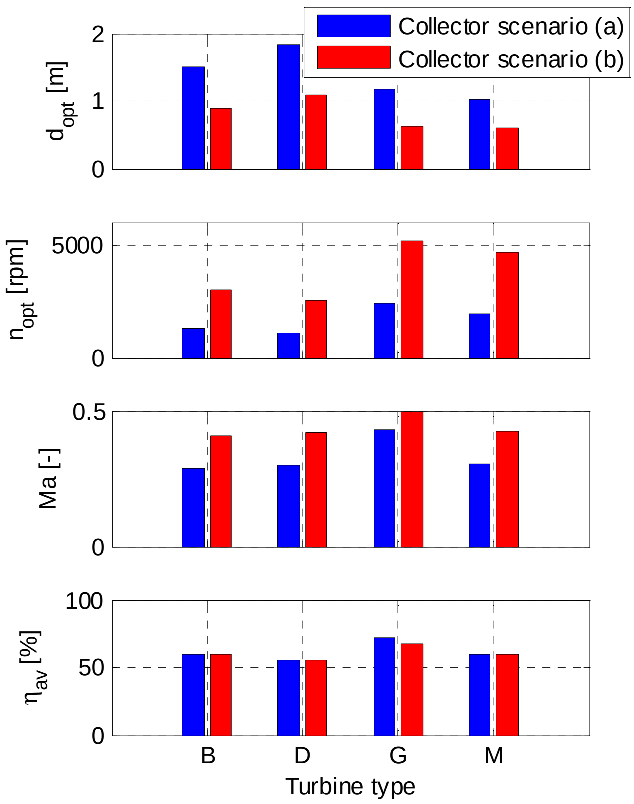

Fig. 10. All turbine types in the catalogue: Optimal parameters and average efficiency.

power point, i.e. the turbine will tolerate sea states with considerably higher pressure amplitude without stalling. The opposite is true for G. This turbine operates close to its maximum power point or even at. Hence, D does not necessarily need a speed control, whereas G requires higher speeds for higher sea states. This, however, would violate the critical Ma number criterion and reduce energy yield and increase sound emission.

Tab. 3: Comparison of optimal turbine parameters.

Collector scenario	turbine type	d [m]	n [rpm]	η_{av} [%]	Ma [-]
(a)	D	1.83	1070	55%	0.28
	G	1.18	2430	**72%**	0.43
(b)	D	1.09	2550	55%	0.42
	G	0.63	5170	68%	**0.50**

B. Effect of two turbines in series or parallel

A frequent question is how the turbine size and rotor speed is affected by replacing a single-stage, single-flow turbine by a multi-stage or multi-flow assembly of geometrically similar stages.

Let us analyse turbine type G as single-stage, two-stage and dual-flow assembly for both collector scenarios (a) and (b) from the previous example. Optimal turbine parameters are compiled in Tab. 4. A two stage turbine always requires a larger rotor diameter and lower rotational speed as compared to the single-stage. The opposite is true for the two-flow assembly. Here the critical Mach number can act as a limiter and prevent the turbine from being optimal.

In practice an axial two-stage turbine can easily be assembled in one duct-type housing by arranging two stages in series. A complete stage consisting of rotor and two guide vanes such as turbine G is particular suitable, since the guide vanes provide an inflow velocity profile to the downstream stage similar to the one the upstream stage experiences from free inflow. A two-flow turbine could be derived from radial or diagonal turbines such as turbine M. Alternatively two equal turbines can be flanged to the collector side by side.

Tab. 4: Turbine G: Comparison of optimal turbine parameters for various stage assemblies.

Collector scenario	turbine	d [m]	n [rpm]	η_{av} [%]	Ma [-]
(a)	single-stage	1.18	2430	72	0.43
	two-stage	1.40	1450	72	0.30
	double-flow	0.83	3440	72	0.43
(b)	single-stage	0.63	5170	**68**	**0.50**
	two-stage	0.83	3440	72	0.43
	double-flow	0.45	7310	**68**	**0.50**

IV. CONCLUSIONS

We have described a simple strategy for selecting a turbine for an application in an oscillating water column (OWC) system for a specified design sea state. Starting point was a catalogue of non-dimensional steady-state performance characteristics of various types of turbines. Utilizing standard scaling laws and a simplistic time domain model for the cyclic turbine operation, optimal size, rotor speed of turbines and number of turbines in series or parallel could be determined that

(i) meet the specification of the impedance ('damping') of the OWC-collector outlet for best collector performance,
(ii) is able to process the pneumatic power, available at the collector outlet
(iii) yield maximum energy over a wave cycle.

A simple example illustrated the application of the method.

In this paper the optimal size and rotational speed of each turbine type considered were identified on the basis of only one sea state, the 'design' sea state. In reality this could be the sea state which is dominant in a particular wave climate. Of course, the performance of any optimal turbine needs to be assessed for all other sea states encountered at a specific site. Maximizing of the overall energy yield may require modifications.

The method can easily be extended to include a hysteresis in the steady-state turbine performance curves (a peculiarity of most turbine types, if they are operated beyond their stall margin), asymmetric turbine performance or asymmetric available power from the collector. Moreover, if acoustic emission characteristics are available (as for all the turbines developed and tested at the University of Siegen [15]), the turbine sound emission can be taken into account as well.

Finally, the effect of an optional speed control strategy on the effective performance characteristic can be included. Given the optimal turbine for the 'design' sea state, often the turbine speed is adapted when the turbine is facing off-design sea states with different pressure amplitudes or time periods. The discussion of speed control strategies is not within the scope of this paper. It is worth to mention, however, that for any turbine type, as long as its working principle is based on change of momentum (in contrast to positive displacement) and the variation of Mach and Reynolds number are moderate, the fundamental scaling laws

$$\dot{V} \propto n \text{ and} \quad (13)$$

$$\Delta p_{ts} \propto n^2 \quad (14)$$

hold true. This inevitably implies that the slope of the characteristic $\dot{V} = f\left(\Delta p_{ts}\right)$ becomes less steep as the rotational speed is increased. The graph in Fig. 11 illustrates this effect on the basis of turbine G. Resolving eqs. (3) and (4) for $\dot{V}$ and Δp_{ts} allows to express the damping eq. (1) in terms of relevant variables:

$$D_{ts} = \frac{\psi_{ts}}{\varphi}\frac{2\rho}{d}n \quad (15)$$

Obviously, given the turbine type (ψ_{ts}/φ) and its rotor size d, the damping D_{ts} is increasing linearly with n. The smaller d und the larger ψ_{ts}/φ, the more the damping is affected by a variation of speed. This is why the damping provided by turbines G or M from our catalogue is much more sensitive to a variation of rotor speed than for instance by type D. In case an OWC-collector requires variable damping, say as a function of sea state, one could take advantage of this effect by implementing the appropriate control strategy for the rotor speed.

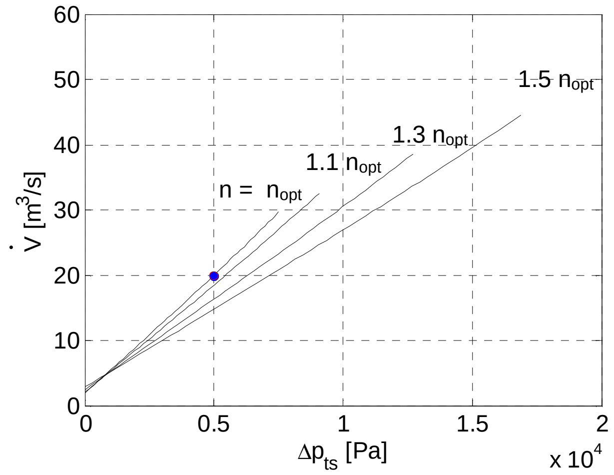

Fig. 11. Effect of the variation of rotational speed on performance curves (optimal turbine G for a 'design' damping D_{ts} = 250 Pa/(m3/s))

ACKNOWLEDGMENT

This work is supported by Voith Hydro, Heidenheim, Germany and the German Federal Ministry for the Economics and Energy and (FKZ 0325396). The authors greatly appreciate this support. We also want to thank Dipl.-Ing. B. Homrighausen for his countless hours of 3D CAD work. Without this work the precise CNC-manufacture of the many model scale turbines designed and tested at the University of Siegen would not have been possible.

REFERENCES

[1] Wells, A. A., Fluid driven rotary transducer, *British Patent Spec No. 159570.*, 1976.

[2] Raghunathan, S., "The Wells air turbine for wave energy-conversion," *Progress in Aerospace Sciences*, vol. 31, pp. 335-386, 1995.

[3] Moisel, C., Starzmann, R., Experimental investigation of different stator vane designs for Well turbines. *Internal report No. B29 100 014A of the Institute of Fluid- and Thermodynamics, University of Siegen*, 2011

[4] Starzmann, R., Carolus, Th., Model-based selection of full-scale Wells turbines for ocean wave energy conversion and prediction of their aerodynamic and acoustic performances. *Proc IMechE, Part A: J Power and Energy* 2014, Vol 228(1) 2-16

[5] Starzmann, R., Aero-acoustic analysis of Wells turbines for ocean wave energy conversion. *Fortschritt-Bericht VDI Reihe 7* Nr. 500, VDI-Verlag, 2012

[6] Starzmann, R., Carolus, Th.: Effect of blade skew strategies on the operating range and aeroacoustic performance of the Wells turbine. *ASME Journal of Turbomachinery*, Jan 2014, Vol. 136, 1-11

[7] Starzmann, R., Guide vanes for Wells turbines: A summary of investigations. *Internal report no. B10 002A of the Institute for Fluid- und Thermodynamics, University of Siegen*, Jan. 2012

[8] Moisel, C., Carolus, Th.: Radial lift-based cascade for bi-directional wave energy air-turbines. *Proc. of the ASME Turbo Expo 2014*, GT2014-25821, 2014

[9] Moisel, C., Carolus, Th., Novel bidirectional mixed-flow air-turbine for wave energy conversion. *11th European Wave and Tidal Energy Conference*, Nantes, France, 2015

[10] Babinstev, I. A., Apparatus for converting sea wave energy into electrical energy, *US Patent No. 3922739*, 1975

[11] Setoguchi, T., Takao, M., Current status of self rectifying air turbines for wave energy conversion, *Energy Conversion and Management*, Vol. 47, pp. 2382-2396, 2006
[12] Falcão, A. F. O., Gato, L. M. C., Air Turbines, in *Comprehensive Renewable Energy*. vol. 8, A. Sayigh (Ed.), Oxford: Elsevier, 2012, pp. 111-149
[13] Curran, R. and Folley, M., Air turbine design for OWCs, in *Ocean Wave Energy: Current Status and Future Perspectives*, J. Cruz (Ed.), Berlin: Springer-Verlag, 2008
[14] Carolus, Th., A data base of bidirectional air turbines. *Internal report No. B00 100 02A of the Institute of Fluid- and Thermodynamics, University of Siegen*, 2015